

## Accepted Manuscript

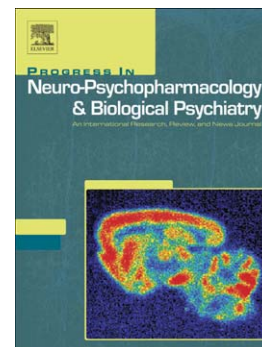
Abnormal Topological Organization in White Matter Structural Networks Revealed by Diffusion Tensor Tractography in Unmedicated Patients With Obsessive-compulsive Disorder

Zhao Xi Zhong, Teng Da Zhao, Jia Luo, Zhi Hua Guo, Meng Guo, Ping Li, Jing Sun, Yong He, Zhan Jiang Li

PII: S0278-5846(14)00006-2  
DOI: doi: [10.1016/j.pnpbp.2014.01.005](https://doi.org/10.1016/j.pnpbp.2014.01.005)  
Reference: PNP 8540

To appear in: *Progress in Neuropsychopharmacology & Biological Psychiatry*

Received date: 26 September 2013  
Revised date: 6 January 2014  
Accepted date: 7 January 2014



Please cite this article as: Zhong Zhao Xi, Da Zhao Teng, Luo Jia, Guo Zhi Hua, Guo Meng, Li Ping, Sun Jing, He Yong, Li Zhan Jiang, Abnormal Topological Organization in White Matter Structural Networks Revealed by Diffusion Tensor Tractography in Unmedicated Patients With Obsessive-compulsive Disorder, *Progress in Neuropsychopharmacology & Biological Psychiatry* (2014), doi: [10.1016/j.pnpbp.2014.01.005](https://doi.org/10.1016/j.pnpbp.2014.01.005)

This is a PDF file of an unedited manuscript that has been accepted for publication. As a service to our customers we are providing this early version of the manuscript. The manuscript will undergo copyediting, typesetting, and review of the resulting proof before it is published in its final form. Please note that during the production process errors may be discovered which could affect the content, and all legal disclaimers that apply to the journal pertain.

**Abnormal Topological Organization in White Matter Structural  
Networks Revealed by Diffusion Tensor Tractography in  
Unmedicated Patients With Obsessive-compulsive Disorder**

Zhao Xi Zhong,<sup>1</sup> Teng Da Zhao,<sup>2</sup> Jia Luo,<sup>1</sup> Zhi Hua Guo,<sup>1</sup> Meng Guo,<sup>1</sup> Ping Li,<sup>1</sup> Jing Sun,<sup>3</sup> Yong He,<sup>2</sup> Zhan Jiang Li<sup>1</sup>

**Correspondence should be addressed to either of the following:**

Zhan Jiang Li, MD, PhD

Department of Clinical Psychology, Beijing Anding Hospital,

Capital Medical University, Beijing 100088, China

Tel: +86 10 58 303 004; Fax: + 86 10 58 303 004

Email: lizhj8@ccmu.edu.cn

Dr Yong He

State Key Laboratory of Cognitive Neuroscience and Learning,

Beijing Normal University, Beijing 100875, China.

Email: yong.he@bnu.edu.cn.

---

<sup>1</sup> Department of Clinical Psychology, Beijing Key Laboratory for Mental Disorders, Beijing Anding Hospital, Capital Medical University, Beijing 100088, China.

<sup>2</sup> State Key Laboratory of Cognitive Neuroscience and Learning, Beijing Normal University, Beijing 100875, China.

<sup>3</sup> School of Medicine and Griffith Health Institute, Griffith University, Q4222, Australia

## Abstract

**Background:** Obsessive-compulsive disorder (OCD) is a chronic psychiatric disorder defined by recurrent thoughts, intrusive and distressing impulses, or images and ritualistic behaviors. Although focal diverse regional abnormalities white matter integrity in specific brain regions have been widely studied in populations with OCD, alterations in the structural connectivities among them remain poorly understood. **Objective:** The aim was to investigate the **abnormalities** in the topological efficiency of the white matter networks and the correlation between the network metrics and Yale-Brown Obsessive-Compulsive Scale scores in unmedicated OCD patients, using diffusion tensor tractography and graph theoretical approaches. **Methods:** This study used diffusion tensor imaging and deterministic tractography to map the white matter structural networks in 26 OCD patients and 39 age- and gender-matched healthy controls; and then applied graph theoretical methods to investigate **abnormalities** in the global and regional properties of the white matter network in these patients. **Results:** The patients and control participants both showed small-world organization of the white matter networks. However, the OCD patients exhibited significant **abnormal** global topology, including decreases in global efficiency ( $t=-2.32$ ,  $p=0.02$ ) and increases in shortest path length,  $L_p$  ( $t=2.30$ ,  $p=0.02$ ), the normalized weighted shortest path length,  $\lambda$  ( $t=2.08$ ,  $p=0.04$ ), and the normalized clustering coefficient,  $\gamma$  ( $t=2.26$ ,  $p=0.03$ ), of their white matter structural networks compared with healthy controls. Further, the OCD patients showed a reduction in nodal efficiency predominately in the frontal regions, the parietal regions and caudate nucleus. The normalized weighted shortest path length of the network metrics was significantly negatively correlated with obsessive subscale of the Yale-Brown Obsessive-Compulsive Scale ( $r=-0.57$ ,  $p=0.0058$ ). **Conclusions:** These findings demonstrate the abnormal topological efficiency in the white matter networks in OCD patients.

### Highlights

- Little is known about the topological organization of the white matter networks in OCD patients.
- This study mapped the white matter structural networks and investigated properties in 26 patients and 39 controls.
- Patients showed significantly decreased global efficiencies and nodal efficiency in some brain areas.
- The **abnormalities** of the network metrics were significantly correlated with the Y-BOCS scores.
- A topology-based brain network analysis can study the structural connectivities in an OCD brain.

**[Keywords]** brain network; connectivity; diffusion tensor imaging; Obsessive-compulsive disorder

**Abbreviations:** OCD, Obsessive-compulsive disorder; WM, white matter; Y-BOCS, Yale-Brown Obsessive-Compulsive Scale; Y-BOCS1, Obsessive subscale of Yale-Brown Obsessive-Compulsive Scale; Y-BOCS2, Compulsive subscale of Yale-Brown Obsessive-Compulsive Scale; DTI, diffusion tensor imaging; DSM-IV, Diagnostic and Statistical Manual of Mental Disorders; OFC, orbito-frontal cortex; MRI, Magnetic Resonance Imaging; PFC, prefrontal cortex; HCs, health controls; FA, fractional anisotropy; ROI, region of interest; VBM, Voxel-based morphometry; AAL, automated anatomical labeling; MDD, major depression disorder;  $S_p$ , Network Strength;  $E_{glob}$ , Network global efficiency;  $E_{loc}$ , Network local efficiency;  $L_p$ , the shortest path length;  $C_p$ , the clustering coefficient;  $\lambda$ , the normalized shortest path length;  $\gamma$ , the normalized clustering coefficient;  $\sigma$ , small-worldness;

## 1. Introduction

Obsessive-compulsive disorder (OCD) is a chronic psychiatric disorder defined by recurrent thoughts, intrusive and distressing impulses or images (obsessions), and ritualistic behaviors and mental acts (compulsions) that are used to reduce the anxiety associated with the obsessive thoughts. OCD is often associated with significant anxiety, distress and social dysfunction (Weissman et al., 1994). The worldwide prevalence of this disorder is 2% to 3% (Horwath and Weissman, 2000), and the mean onset age is usually late adolescence (Taylor, 2011). The pathogenesis of OCD is largely unknown, though genetic factors may play an important role. A family-based genetic association study reported biased transmission of alleles of the MOG gene (myelin oligodendrocyte glycoprotein gene) in OCD patients (Zai et al., 2004). MOG is a cellular adhesion molecule of oligodendrocyte, which serves as an important part of the white matter (myelin). Bilateral orbitomedial leucotomy for one patient with severe and intractable OCD also showed remarkable improvement in obsessive-compulsive symptoms (Sachdev et al., 2001). All these studies suggest that the structural and functional defect(s) of white matter (WM) may be a vital neurobiological basis in the pathogenesis of OCD. Several studies have also revealed that WM alterations are associated with greater severity of obsessive-compulsive symptoms. In Magnetic Resonance Imaging (MRI) morphometric studies, Garber et al. (1989) found that right-minus-left T1 differences in the orbital PFC cortex were strongly correlated with symptom severity in OCD patients. Duran et al. (2009) found patients' symptom severity scores demonstrated positive correlations with volumes of large bilateral clusters of WM volume in the anterior limb of internal capsule. Magnetic resonance spectroscopy (MRS) studies found OCD patients exhibited neurochemical abnormalities in the frontal (Whiteside et al., 2006) and parietal (Kitamura et al., 2006) WM that correlated positively with the severity of symptoms.

Diffusion tensor imaging (DTI) is a noninvasive imaging technique that can be used to investigate WM microstructures. In recent years, several DTI studies have shown

that OCD patients exhibited diverse regional abnormality in WM integrity in different brain regions of OCD patients. In these studies, Szeszko et al. (2005) observed that patients exhibited significantly lower fractional anisotropy (FA) bilaterally in three areas of the anterior cingulate cortex, parietal region (supramarginal gyri), right posterior cingulated gyrus, and left occipital lobe (lingual gyrus). Subsequently, Cannistraro et al. (2007) found significantly greater FA in the cingulate bundle bilaterally and in the left anterior limb of the internal capsule of patients. Lochner et al. (2012) also found patients showed increased FA in bilateral regions of the anterior limb of the internal capsule, as well as decreased FA in the right anterior limb near the head of the caudate. Saito et al. (2008) observed a significant reduction in FA in the rostrum of the corpus callosum of patients, while Garibotto et al. (2010) found patients showed significantly lower FA in corpus callosum, cingulum, superior longitudinal fasciculus, and inferior fronto-occipital fasciculus bilaterally. In another study, Li et al. (2011) found OCD patients demonstrated significantly increased FA in the genu and body of corpus callosum and WM of the right superior frontal gyrus (SFG) and corpus callosum. Fan et al. (2012) found patients showed significantly decreased FA in the left medial SFG, temporo-parietal lobe and middle occipital gyrus and around the left striatum WM. These studies provide a potential mechanism of the structural disconnections in the brain of OCD patients.

Previous findings regarding WM alterations in OCD patients were rather heterogeneous. These heterogeneous findings may in part stem from difficulties in anatomically registering DTI data, and may well suggest that OCD is associated with large-scale disruption in brain systems or networks, as opposed to being a consequence of disturbances in isolated brain regions (Fontenelle et al., 2009). The human brain is a complex organ, and it is the activity of the connected cellular ensembles that stores the memories, produces the thoughts, and drives the actions (Sporns et al., 2005). Therefore, it is better to investigate the brain functions from the perspective of connected cellular networks. Network-based measures can consider each region's integration into the global unit rather than as an independent entity;

therefore, such measures are more sensitive to alterations that are not apparent in gross isolated structures (Zalesky et al., 2010). However, very little is known about alterations in the topological organization of the WM networks in OCD patients.

This study used DTI tractography and graph theoretical approaches to investigate abnormalities in the topological organization of the WM networks in OCD patients. Tractography is a novel 3D modeling technique used to visually represent neural tracts using data collected by DTI. Tractography is a useful tool for measuring deficits in WM, such as reliable estimation of fiber orientation and strength. It is currently a primary methodology for characterizing the brain's WM or "structural" network. The graph theoretical approach serves as an effective methodology to analyze the connections of the brain networks (Bullmore and Sporns, 2009; He and Evans, 2010).

This study hypothesized that: (1) OCD patients would show an abnormal topological pattern revealed by global and regional characteristics in the WM networks; and (2) these abnormal topological metrics would correlate with quantitative clinical symptomatic measurements, such as the Yale-Brown Obsessive-Compulsive Scale (Y-BOCS) scores.

## **2. Materials and Methods**

### **2.1 Participants**

The present study included 26 OCD outpatients (female/male: 9/17; mean age:  $28.8 \pm 7.6$  years) and 39 health controls (HCs) (female/male: 13/26; mean age:  $27.7 \pm 7.7$ ). All patients met the DSM-IV (1994) diagnostic criteria for OCD, using the Structured Clinical Interview for DSM-IV Axis I disorders. Patients were diagnosed by two experienced senior psychiatrists. All the participating patients visited an outpatient clinic at Capital Medical University, Beijing Anding Hospital, China, from October 2009 to August 2011. The Y-BOCS (Goodman et al., 1989) was used to assess illness severity. Only patients with a score  $\geq 16$  on the Y-BOCS scale were

included. Every patient also received the 17-item Hamilton Depression Rating Scale (HAMD) (Hamilton, 1960) and the 14-item Hamilton Anxiety Rating Scale (HAMA) (Hamilton, 1959) to assess the severity of depression and anxiety, respectively. Other inclusion criteria were: (i) never used psychiatric medication before the study; (ii) between 18 and 50 years old; (iii) right-handed; (iv) no history of neurological illness or other major physical diseases; (v) no history of other major psychiatric disorders such as schizophrenia, mood disorders; (vi) no history of psychoactive substances, alcohol dependence and/or abuse.

The study recruited 39 healthy volunteers from the local community using the Structured Clinical Interview for Diagnostic and Statistical Manual of Mental Disorders, 4th ed. Axis I Disorders-Non-patient Edition. The controls were matched for age, sex, and handedness with patients. None of the healthy controls had any neurological and psychiatric illnesses, major physical diseases, or positive family history of major psychiatric disorders. The detailed clinical and demographic data for all participants are shown in Table 1. This study was approved by the Research Ethics Committee at Beijing Anding Hospital, Capital Medical University. All participants were remunerated for their work. Written informed consent was obtained from all participants.

## **2.2 Brain Image Acquisition**

All participants were scanned with a SIEMENS 3-T scanner (Tim Systems) at the State Key Laboratory of Cognitive Neuroscience and Learning, Beijing Normal University, China. Participants lay supine with foam pads and ear plugs to minimize head motion. Diffusion-weighted images were acquired with an Echo-Planar Imaging-based sequence covering the whole brain. The acquisition parameters were as follows: time repetition (TR)=7200ms; echo time (TE)=104ms; number of excitations (NEX)=8; in-plane acquisition matrix=128x128; field of view (FOV)=230x230mm<sup>2</sup>; 2.5-mm slice thickness with no interslice gap; and 49 axial

slices. The diffusion sensitizing gradients were applied along 64 noncollinear directions ( $b=1000\text{s/mm}^2$ ), together with an acquisition without diffusion weighted ( $b=0\text{s/mm}^2$ ). High-resolution T1-weighted images were obtained by GR\IR sequence as follows: TR=2530ms; TE=3.39ms; time to inversion=1100ms; flip angle=15°; in-plane acquisition matrix=169x196; FOV=169x196mm<sup>2</sup>; 1.33mm slice thickness with no interslice gap; and 169 axial slices.

### 2.2.1 Brain Imaging Data Preprocessing

The data preprocessing consisted of several steps. First, the distortion of diffusion-weighted images due to eddy currents and motion artifacts were corrected using an affine registration (FSL; <http://www.fmrib.ox.ac.uk/fsl>). Second, the diffusion tensor model was fitted and the tensor matrix was diagonalized to obtain three eigenvalues and eigenvectors voxel by voxel. The FA value of each voxel was based on computed eigenvalues (DTI studio; <http://lbam.med.jhmi.edu>). Last, the whole brain fiber tracking was performed via the Fiber Assignment by Continuous Tracking (FACT) algorithm by seeding from the center of each voxel, with the FA threshold of 0.2 and tracking turning angular threshold of 45° (Mori et al., 1999).

### 2.2.2 Brain Network Construction

The whole brain fiber bundles linked different cortical regions form a huge complicated network. The most basic element network nodes and edges are defined as follows.

#### 2.2.2.1 Network Node Definition

This study employed the automated anatomical labeling (AAL) template (Tzourio-Mazoyer et al., 2002) to parcellate the cerebral cortex into 90 cortical

regions (see Figure 1). In order to obtain comparable region of interest (ROI) across participants, the following parcellation process was conducted using SPM8 software (<http://www.fil.ion.ucl.ac.uk/spm/software/spm8>). Briefly, the structural images of each individual participant were coregistered to their non-diffusion-weighted (b0) images and resliced into the DTI space using a linear transformation. The resliced structural images were then nonlinearly transformed into the ICBM152 T1 template in the Montreal Neurological Institute (MNI) space. The transformation matrix was then inverted and used to warp the AAL labels from the MNI space to a DTI native space (Tzourio-Mazoyer et al., 2002) by using nearest-neighbor interpolation to preserve the discrete labeling values (see Figure 1). After this procedure, 90 cortical and subcortical regions (45 for each hemisphere) were obtained (see Table 2), each representing a node of the network (see Figure 1). The spatial scale of the nodal parcellation of the brain network is an intrinsic factor that determines the network topological properties (Van den Heuvel et al., 2008; Wang et al., 2009; Zalesky et al., 2010). Recent studies have shown different parcellation methods to characterize WM network topological structure (Hagmann et al. 2008; Van den Heuvel et al., 2008). Therefore, the AAL template was further subdivided into 1024 ROIs with equal size using a previously described method (Zalesky et al., 2010).

#### 2.2.2.2 *Network Edge Definition*

All the reconstructed fiber bundles in native space were taken into account for the composition of the network edge. For the AAL atlas parcellation, cortical regions were considered structurally connected if at least three fibers with both end points were located in respective region (Shu et al., 2011). A minimum of three fibers was selected as a threshold to reduce the false-positive connections due to the sensitivity to noise in deterministic tractography; and simultaneously to ensure the detection of the largest connected component (Li et al., 2009; Shu et al., 2009) in the prospective network. The number of the connected fibers (FN) between two regions was defined as the weights of the network edges. As a result, the FN-weighted WM network was

constructed for each participant, which was represented by a symmetric 90x90 matrix (see Figure 1). For the high-resolution (1024) network, the same definition of the each edge was considered. The number of interconnecting fibers between two regions was defined as the edge weight. Therefore, a symmetric 1024x1024 matrix was obtained for each participant.

### 2.2.3 Brain Network Analysis

Network metrics for each participant were quantified using GRETNA (<http://www.nitrc.org/projects/gretna/>). For each network, the following metrics were calculated.

#### 2.2.3.1 *Network Strength*

For a network  $G$  with  $N$  nodes and  $K$  edges, the strength of  $G$  was defined as:

$$S_p(G) = \frac{1}{N} \sum_{i \in G} S(i)$$

where  $S(i)$  is the sum of the edge weights  $w_{ij}$  ( $w_{ij}$  are the FN values for the weighted networks) linking to node  $i$ . The strength of a network is the average of the strength of each node in the network.

#### 2.2.3.2 *Weighted Network Cost*

The network cost reflects the expense for holding the connections of a graph and has an opposite effect on network efficiency (Gong et al., 2009). In order to normalize interindividual different cost effects, the weights of each network were divided by its cost. The cost was computed as follows:

$$\text{Cost} = \frac{1}{\text{weight}}$$

### 2.2.3.3 Small-world Properties

Small-world properties (clustering coefficient,  $C_p$ , and shortest path length,  $L_p$ ) were originally proposed by Watts and Strogatz (1998) to characterize an optimized connect pattern of the brain according to evolution and development, which exhibits a balance of regular networks and random networks, possessing high clustering coefficients and low path lengths. The clustering coefficient of a node  $i$ ,  $C(i)$ , which was defined as the possibility of the neighborhoods, connected with each other or not, was computed as follows:

$$C(i) = \frac{2}{k_i(k_i - 1)} \sum_{j,k} (\bar{w}_{ij} \bar{w}_{jk} \bar{w}_{ki})^{1/3}$$

where  $k_i$  is the degree of node  $i$  and  $\bar{w}$  is the weight. The clustering coefficient,  $C_p$ , of a network is the average of the clustering coefficient of each node and indicates the extent of the local interconnectivity or cliquishness in a network.

The path length between any pair of nodes (e.g., node  $i$  and node  $j$ ) is defined as the sum of the edge lengths along this path. For weighted networks, the length of each edge was assigned by computing the reciprocal of the edge weight,  $1/w_{ij}$ . The shortest path length,  $L_{ij}$ , is defined as the length of the path for node  $i$  and node  $j$  with the shortest length. The shortest path length of a network was computed as follows:

$$L_p(G) = \frac{1}{N(N-1)} \sum_{i \neq j \in G} L_{ij}$$

where  $N$  is the number of nodes in the network. The  $L_p$  of a network quantifies the ability for information to propagate in parallel.

A network can be categorized as a small-world network if it has a much higher  $C_p$  and a similar  $L_p$  compared with 100 matched random networks. The matched random networks were generated using the random rewiring procedure, described by Maslov and Sneppen (2002), that preserves the same number of nodes, edges, and degree

distribution as real networks. This study retained the weight of each edge during the random rewiring procedure so that the weight distribution of the network was also preserved. Further, the normalized shortest path length,  $\lambda$  (lambda),  $\lambda = L_p^{real} / L_p^{rand}$  and the normalized clustering coefficient,  $\gamma$  (gamma),  $\gamma = C_p^{real} / C_p^{rand}$ , were computed, where  $L_p^{rand}$  and  $C_p^{rand}$  are the mean clustering coefficient and the mean shortest path length of 100 matched random networks, respectively. These two measurements can be summarized into a simple quantitative metric, small-worldness  $\sigma$  (sigma), which is typically  $>1$  for small-world networks (Humphries et al., 2005).

#### 2.2.3.4 Network Efficiency

The global efficiency of the parallel information transfer in the network (Latora and Marchiori, 2001) can be computed as follows:

$$E_{glob}(G) = \frac{1}{N(N-1)} \sum_{i \neq j \in G} \frac{1}{L_{ij}}$$

where  $L_{ij}$  is the shortest path length between node  $i$  and node  $j$  in  $G$ . The local efficiency reveals how much the network is fault tolerant and shows how efficient communication is among the first neighbors of the node  $i$  when it is removed.

The local efficiency of a graph is defined as follows:

$$E_{loc}(G) = \frac{1}{N} \sum_{i \in G} E_{glob}(G_i)$$

where  $G_i$  denotes the subgraph composed of the nearest neighbors of node  $i$ .

#### 2.2.3.5 Regional Characteristics

To determine the regional characteristics of the WM networks, the nodal strength and efficiency were computed. The nodal strength  $S(i)$  is defined as the sum of all of the

edge weights between this node and all of the other nodes in the network. The nodal efficiency,  $E_{\text{nodal}}(i)$ , is defined as follows (Achard and Bullmore, 2007):

$$E_{\text{nodal}}(i) = \frac{1}{N-1} \sum_{j \in G, j \neq i} \frac{1}{L_{ij}}$$

where  $L_{ij}$  is the shortest path length between node  $i$  and node  $j$ .  $E_{\text{nodal}}(i)$  measures the average shortest path length between a given node  $i$  and all of the other nodes in the network. The node  $i$  is a brain hub if  $E_{\text{nodal}}(i)$  is at least 1 SD greater than the average nodal efficiency of the network.

### 2.3 Statistical Analyses

Data were normally distributed and checked for sphericity. To determine the between-group differences in different global network metrics, linear regression analysis was performed. Age, gender, level of highest diploma, and brain size of each participant were taken as covariates at  $p < 0.05$ , **we also explored results at a more liberal statistical threshold of  $p < 0.01$ , uncorrected.** Likewise, such a linear regression and consideration of covariates was also applied to nodal efficiency. A false discovery rate (FDR) procedure was further performed at a  $q$  value of 0.05 to correct for multiple comparisons. The relationship between the global network metrics and region efficiency, which showed significant group difference, and the Y-BOCS scores in OCD groups using a partial correlation analyses, was further examined. This involved age, gender, level of highest diploma, and brain size as covariates.

## 3. Results

### 3.1 Small-world Properties of WM Networks

A small-world network is a highly optimized system characterized by high local clustering and approximate high global efficiency compared with the matched random networks as expressed by  $\gamma > 1$  and  $\lambda \approx 1$  (Watts and Strogatz, 1998). Compared with a

random network, which preserves the same number of nodes, edges, and degree distribution as the real network (Maslov and Sneppen, 2002; Sporns and Zwi, 2004), results showed that the WM network had a small-world organization in both of the OCD patients [ $\lambda=1.16$  (0.03)  $\gamma=4.32$  (0.38)] and control participants [ $\lambda=1.15$  (0.03)  $\gamma=4.15$  (0.29)] (see Table 3 and Figure 2).

### 3.2 Global Topology Measures of the WM Structural Networks

For each participant, the strength, global, and local efficiency, clustering coefficient, and shortest path length of the WM networks was calculated. Using linear regression analysis with age, gender, educational attainment, and brain size as the covariates, it was found that the OCD patients exhibited significant decreases in global efficiency ( $t=-2.32$ ,  $p=0.02$ ) and increases in shortest path length,  $L_p$  ( $t=2.30$ ,  $p=0.02$ ), normalized weighted shortest path length,  $\lambda$  ( $t=2.08$ ,  $p=0.04$ ), and normalized clustering coefficient,  $\gamma$  ( $t=2.26$ ,  $p=0.03$ ), of their AAL-based WM structural networks compared to the controls (see Table 3 and Figure 2). However, no significant result of global topology measures was found in high-resolution WM network.

### 3.3 Regional Nodal Characteristics of the WM Networks

#### 3.3.1 Hub Regions

The regions were defined as network hubs if their nodal efficiency was 1 SD greater than the average of the network. The study identified 13 hub nodes of the WM structural networks in the normal control group, including 10 association cortex regions and three primary cortex regions, and 14 hub nodes in the OCD group, including 10 association cortex regions and four primary cortex regions. In both groups, 12 brain regions were identified as hubs in common, including the bilateral precuneus (PCUN), bilateral middle temporal gyrus (MTG), bilateral postcentral gyrus (PoCG), bilateral dorsolateral SFG (SFGdor), bilateral supplementary motor area (SMA), right precentral gyrus, and left MOG. In addition, one brain region, the

right middle frontal gyrus (MFG), was identified as a hub in the normal control group but not in the OCD group. Two brain regions, the left MFG and left precentral gyrus (PreCG), were identified as hubs in the OCD group but not in the normal control group (see Figure 3). These results are consistent with those from previous studies (Hagmann et al., 2008; Gong et al., 2009).

### 3.3.2 Group Differences in Regional Efficiency

#### 3.3.2.1 AAL-based Structural Brain Networks

The study further compared the nodal strength and efficiency of cortical regions in WM networks between the two groups. Compared with the controls, the OCD patients showed reduced nodal efficiency ( $p < 0.05$ , FDR corrected) in the right MFG (MFG.R) and right PreCG (PreCG.R) (see Figure 4).

#### 3.3.2.2 High-resolution Structural Brain Networks

As in the AAL network, a similar analysis was also performed in the high-resolution networks. The study found comparable results with AAL network analyses in regional efficiency **abnormalities**. The OCD patients showed reduced nodal efficiency ( $p < 0.01$  uncorrected) in the frontal region (MFG.R, MFG.L, right superior frontal gyrus, medial), PreCG.R and MOG.L, left posterior cingulate gyrus (PCG.L), left caudate nucleus (CAU.L), and MTG.L (see Figure 5).

### 3.4 Correlation between the Network Metrics and Y-BOCS Scores

The study examined the correlation between the four global network metrics, which showed significant group differences (global efficiency, shortest path length, normalized weighted shortest path length, and normalized clustering coefficient), and Y-BOCS scores using a partial correlation analyses in the OCD group at  $p < 0.01$ . It was found that the normalized weighted shortest path length was significantly

negatively correlated with Y-BOCS1 (obsessive subscale) ( $r=-0.57$ ,  $p=0.0058$ ) (see Figure 6). Such a correlation analysis was also used on the nodal efficiency in the abnormal regions and Y-BOCS scores; no significant relationship was found between them, both in low and high-resolution structural brain networks.

#### 4. Discussion

Using DTI and graph theory methods, the topological **abnormalities** of WM networks in OCD patients are shown.

##### 4.1 Disrupted Global Topological Organization in the WM Networks in OCD

In this study, it was found that WM networks in both OCD patients and healthy controls showed small-world properties. However, some network properties, including global efficiencies, shortest path length, normalized weighted shortest path length, and normalized clustering coefficient, were significantly abnormal in the OCD patients compared with controls. OCD patients exhibited significant decreases in global efficiency and increases in shortest path length, normalized weighted shortest path length, and normalized clustering coefficient. Global efficiency is known to reflect the ability to transfer information between different nodes of a network; and it is a comprehensive index for the parallel information processing capabilities. Short path lengths ensure interregional effective integrity or prompt transfer of information in brain networks, which constitutes the basis of cognitive processes (Latora and Marchiori, 2001). The degeneration of fiber bundles can lead to increases in the short path lengths. Decreases in global efficiencies and increases in short path lengths could be attributable to the degeneration of fiber bundles for information transmission.

These phenomena suggest that the connections between cortical areas **are abnormal** with less strength (reduced WM integrity) or longer pathways (disconnection). The normalized shortest path length was compared to a random network. The abnormality

indicates dysfunction of **brain optimal balance between local specialization and global integration, which can support both segregated/specialized and distributed/integrated information processing are dysfunctional in OCD patients.**

The normalized clustering coefficient is a comparison between local information transmission capability and random networks. The increases in the normalized weighted shortest path length and the normalized clustering coefficient reflect a strengthening of information transmission capability in patients' brains. Therefore, the results suggest that some information may be constrained in some areas, which leads to over expression, and not transmitted to other larger areas, which leads to under expression of general function.

These results are consistent with the facts of repeated obsession and compulsion while general function decreases in OCD patients. Some DTI studies showed disrupted structural integrity in various WM tracts, including the cingulate fasciculus, the inferior fronto-occipital fasciculus, optic radiation, superior longitudinal fasciculus, thalamic radiations, and the corpus callosum (Cannistraro et al., 2007; Bora et al., 2011; Chiu et al., 2011; Oh et al., 2012). **A functional brain network analysis study using graph theory reported by Zhang et, al. (2011) showed that OCD patients demonstrated a significantly higher clustering coefficient in a ‘top-down control network’ (multiple prefrontal, parietal, temporal, occipital, and subcortical regions) compared to the controls. The study also found that the clustering coefficient correlated with functional connectivity for primarily short-range functional connections. Although Zhang et al.’s (2011) study examined functional rather than structural networks, the current study suggests that OCD patients may show similar patterns of aberrant structural network properties.**

**In another WM brain network analysis study using graph theory, Arienzo et al. (2013) observed that patients with body dysmorphic disorder(BDD), an obsessive-compulsive-related disorder demonstrated a higher whole-brain mean clustering coefficient than controls, and global efficiency was negatively**

**correlated with symptom severity. BDD has similarities to OCD in terms of overlapping phenomenology, shared heredity, and evidence of shared genetics (Monzani et al. 2012).** These results provide support to the findings of this study, which suggest disrupted topological organization of the WM networks in OCD patients. Characterization of the global architecture of the anatomical connectivity patterns in the human brain could increase our understanding of how functional brain states emerge from their underlying structural substrates and provide new insights into the association of brain function deficits with underlying structural disruption in brain disorders (Sporns et al., 2005). As far as it has been ascertained, this study is the first to use diffusion MRI tractography to show small-world **abnormalities** in WM networks in OCD brains.

#### **4.2 Disrupted Nodal Efficiency in the WM Networks in OCD Patients**

It was observed that the OCD patients showed a reduction in the nodal efficiency, predominately in: (1) the frontal regions, right middle frontal gyrus (MFG); (2) the parietal regions—PreCG.R;

A large body of literature supports the existence of parallel circuits linking the basal ganglia, thalamus, and cortex with circuits communicating with separate areas of the frontal cortex (Alexander et al., 1986). Neuropsychological studies have reported that OCD patients show deficits related to frontal cognitive abilities, such as executive functioning and cognitive-behavioral flexibility (Friedlander and Desrocher, 2006). Many previous studies have demonstrated that these frontal association regions exhibit OCD-related abnormalities. Functional imaging studies observed significantly lower regional cerebral glucose metabolic rates in the prefrontal lateral cortex (Martinot et al., 1990) and higher regional cerebral blood flow (rCBF) in the medial-frontal (Machlin et al., 1991) and right and left dorsolateral prefrontals (Diler et al., 2004) in OCD patients than in control groups. Some morphological studies also reported OCD patients had thinner left inferior frontal, left middle frontal and left

precentral (Shin et al., 2007) and showed decreased grey matter as well as decreased WM in bilateral frontal regions (Susanna et al., 2007).

Functional MRI studies have found OCD patients showed significant decreased frontal-striatal responsiveness, mainly in the dorsolateral prefrontal cortex during planning (van den Heuvel et al., 2005) and demonstrated less functional connectivity within the resting state functional connectivity in the default mode network in the MFG (Jang et al., 2010) compared to controls. DTI analysis showed OCD patients demonstrated significantly increased FA in the right SFG (Li et al., 2011) but decreased FA in the left medial SFG (Fan et al., 2012), and a higher apparent diffusion coefficient in the left medial-frontal cortex (Nakamae et al., 2008).

Current knowledge from functional and structural neuroimaging emphasizes abnormalities of fronto-striatal-thalamic-cortical circuits and orbitofronto-striato-thalamic circuits in the pathophysiology of OCD (Saxena et al., 1999; Saxena et al., 2001). This study's findings reflect the WM abnormality of the connections between the frontal regions and other regions. Thus, the results are in agreement with these neurobiological bases.

The parietal cortex is known to be involved in attention and visuospatial processes, as well as various executive functions, such as task switching, planning, and working memory (Posner and Petersen, 1989). Parietal dysfunction may interact with the frontal-subcortical circuits through an anatomical connection between parietal associative areas and the lateral orbitofrontal cortex, the striatum, and the thalamic nucleus (Valente Jr et al., 2005). Parietal dysfunction, such as WM integrity (Szeszko et al., 2005), WM volume (Carmona et al., 2007), grey matter volume (Kim et al., 2001; Valente Jr et al., 2005), and functional alterations related to the symptoms of OCD (Kwon et al., 2009) may contribute to the cognitive impairments found in some OCD patients. This study's results suggest that WM abnormality of the connections in the parietal cortex might influence information transmission in OCD patients.

In high-resolution structural brain networks, the OCD patients showed reduced nodal efficiency in the left caudate nucleus in addition to the above-mentioned regions. The caudate nucleus is also a region of interest in the pathophysiology mechanism of OCD, which has indicated abnormalities in WM integrity (Yoo et al., 2007) and functional alterations (Kwon et al., 2009) in OCD patients. The current results implied an abnormal connection between the caudate nucleus and other brain areas, and further demonstrated abnormalities of fronto-striatal-thalamic-cortical circuits in the pathophysiology of OCD from the perspective of network connections.

Using graph theoretical analysis, this study's results show that the frontal regions, the parietal regions and the caudate nucleus have reduced nodal efficiency in WM networks, which reflects the WM abnormality of the connections in these cortical regions. As stated in the introduction, DTI studies have shown variable FA values in different brain regions, which reflect regional WM integrity abnormalities in these regions of OCD patients. These abnormalities might influence information transmission and lead to the WM abnormality of the connections in these cortical regions. Thus, the current findings are consistent with previous DTI studies, and the reduced nodal efficiency is likely related to the abnormalities of FA values in these regions.

In summary, the results of the graph theoretical analysis showed that there was a decreased topological efficiency in the WM networks in OCD patients. This may infer abnormal WM connections in cortical regions or between them. This study proposes that the abnormal WM integrity may cause the structural and functional **abnormality** in these brain regions, and then causes abnormal structural and functional connectivity in brain networks between regions, which can bring about the symptoms of OCD, such as the weakening of inhibitory ability and repetitive behavior.

#### 4.3 Correlation between the Network Metrics and Y-BOCS Scores

It was found that the normalized weighted shortest path length was significantly negatively correlated with Y-BOCS1 (obsessive subscale). A previous ROI-based study reported significant correlations between Y-BOCS scores and the volume in the regional cerebral cortex, such as left OFC, right OFC, or left thalamus (Atmaca et al., 2007). A previous Voxel-based morphometry (VBM) study reported inverse correlations between Y-BOCS scores and grey matter volume in the thalamus (Valente Jr et al., 2005). Some DTI researches reported significant correlations between the Y-BOCS scores and the FA values in the WM in OCD patients (Fontenelle et al., 2009; Li, Huang et al., 2011). This present study is the first to show the correlation between the Y-BOCS scores and structural organization in OCD patients from a network perspective. It was found that the network metrics (both global efficiency and regional nodal efficiency) of OCD patients were not significantly correlated with Y-BOCS. Interestingly, however, it was found that the normalized weighted shortest path length was significantly negatively correlated with the Y-BOCS obsessive subscale score. The normalized shortest path length was compared to random networks. The abnormality indicates dysfunction of brain balance optimization, so the results suggest that dysfunction of brain WM network balance optimization in OCD patients is highly associated with obsession. Previous studies have demonstrated that the Y-BOCS obsessive subscale score is significantly correlated with the FA values in the WM in OCD patients (Li et al., 2011). Thus, the current results **agree with others studies that suggest that the clinical symptoms of different subtypes of OCD might have abnormal neural correlates and brain connectivity (Mataix-Cols et al., 2004).**

## 5. Limitations

Several limitations must be considered. First, the deterministic tractography used to construct WM networks cannot handle the “fiber crossing” problem (Mori and van Zijl, 2002), which might result in premature termination of tractography. The tensor model that only allows one fiber orientation within a single voxel cannot fit the cross

fiber either. Other methods such as probabilistic tractography (Iturria-Medina et al., 2008; Gong et al., 2009) or models such as the diffusion spectrum MRI could be helpful to address the issues. OCD patients have also been studied using functional MRI data. The combination of different multimodal MRI techniques would yield a more comprehensive view of how aberrant structure connectivity is associated with excessive function in OCD patients.

Second, the sample in this research is relatively small; and the representativeness of the results requires further verification through an enlarged sample size. In this study's sample, the mean age for the OCD group was 28.8 years and the mean illness duration was 4.6 years; thus the mean age of onset was about 24.2 years. However, since only approximately 24% of cases of OCD have their onset after adolescence (Taylor, 2011), this may not represent the general OCD population. The study sample should be increased in the future. In addition, those with a history of other comorbid major psychiatric disorders, including mood disorders, were excluded. Not allowing any comorbid anxiety disorder, major depression disorder (MDD), or dysthymia therefore was a non-representative sample, since, for example, 60% to 80% of people with OCD have a history of MDD. However, in order to protect the homogeneity of the participants and reduce its influence on results, the inclusion and exclusion criteria were constructed. For example, Ajilore et al. (2013) found that MDD patients demonstrated abnormal topological efficiency in WM networks. Moreover, no subjects in this study had ever been treated with psychiatric medication, so this may not represent unusual cases. Medication may have effects on brain structure, so only subjects who had never been treated with psychiatric medications were chosen to control this confounding factor.

Third, studies have shown that the clinical symptoms of different subtypes of OCD might have distinctive neural correlates and brain connectivity (Mataix-Cols et al., 2004). This study did not differentiate the OCD patients into subtypes according to

their clinical symptoms, such as obsessive and compulsive checking, cleaning, compulsive symmetry, and hoarding.

## 6. Conclusion

In this study, DTI tractography and graph theoretical approaches were used to investigate the topological organization of the WM networks in OCD patients. It was found that OCD patients presented significantly decreased global efficiencies in WM networks compared with controls, suggesting disrupted topological organization of the WM networks in OCD patients. The study's OCD patients also showed a reduction in nodal efficiency, predominately in the brain areas of the frontal regions, the parietal regions and the caudate nucleus. Further, these **abnormalities** to the network metrics were significantly correlated with the Y-BOCS scores. The data also suggest that a topology-based brain network analysis can provide an innovative and systematic methodology to study the structural and functional connectivity in OCD brains in order to fully understand of the neurobiology of OCD.

**Contributors**

Zhaoxi Zhong, Zhanjiang Li and Yong He contributed to the conception and design of the study and the acquisition, analysis and interpretation of data. Jia Luo, Zhihua Guo, Meng Guo and Ping Li contributed to the conception and design of the study and the acquisition of data. Teng Da Zhao and Yong He contributed to the conception and design of the study and the analysis of data. Zhaoxi Zhong, Zhanjiang Li and Jing Sun wrote the article, which all other authors reviewed. All authors gave approval for publication.

**Conflict interest**

All authors declare no conflict of interest.

**Role of funding source**

This work was partly supported by National Natural Science Foundation of China Grants 81271493 and Beijing Natural Science Foundation Grant 7122082.

**Acknowledgements**

We thank all the participants and their families and Prof. Kieron O'Connor from University of Montreal for his useful discussion and comments on this manuscript.

## References

Achard S, Bullmore E. Efficiency and cost of economical brain functional networks. *PLoS computational biology*.2007;3(2): e17.

Ajilore O, Lamar M, Kumar A. Association of brain network efficiency with aging, depression, and cognition. *The American Journal of Geriatric Psychiatry*.2013.

Alexander GE, DeLong MR, Strick PL. Parallel organization of functionally segregated circuits linking basal ganglia and cortex. *Annual review of neuroscience*.1986;9(1): 357-81.

Arienzo D, Leow A, Brown JA, Zhan L, GadElkarim J, Hovav S, et al. Abnormal Brain Network Organization in Body Dysmorphic Disorder. *Neuropsychopharmacology*.2013.

Atmaca M, Yildirim H, Ozdemir H, Tezcan E, Kursad Poyraz A. Volumetric MRI study of key brain regions implicated in obsessive–compulsive disorder. *Progress in neuro-psychopharmacology and Biological Psychiatry*.2007;31(1): 46-52.

Bora E, Harrison BJ, Fornito A, Cocchi L, Pujol J, Fontenelle LF, et al. White matter microstructure in patients with obsessive–compulsive disorder. *Journal of psychiatry & neuroscience: JPN*.2011;36(1): 42.

Bullmore E, Sporns O. Complex brain networks: graph theoretical analysis of structural and functional systems. *Nature Reviews Neuroscience*.2009;10(3): 186-98.

Cannistraro PA, Makris N, Howard JD, Wedig MM, Hodge SM, Wilhelm S, et al. A diffusion tensor imaging study of white matter in obsessive–compulsive disorder. *Depression and anxiety*.2007;24(6): 440-6.

Carmona S, Bassas N, Rovira M, Gispert J-D, Soliva J-C, Prado M, et al. Pediatric OCD structural brain deficits in conflict monitoring circuits: a voxel-based morphometry study. *Neuroscience letters*.2007;421(3): 218-23.

Chiu C-H, Lo Y-C, Tang H-S, Liu I, Chiang W-Y, Yeh F-C, et al. White matter abnormalities of fronto-striato-thalamic circuitry in obsessive–compulsive disorder: A study using diffusion spectrum imaging tractography. *Psychiatry Research: Neuroimaging*.2011;192(3): 176-82.

Diler RS, Kibar M, Avci A. Pharmacotherapy and regional cerebral blood flow in children with obsessive compulsive disorder. *Yonsei Medical Journal*.2004;45(1): 90-9.

Duran FLdS, Hoexter MQ, Valente Jr AA, Miguel EC, Busatto Filho G. Association between symptom severity and internal capsule volume in obsessive-compulsive disorder. *Neuroscience letters*.2009;452(1): 68-71.

Fan Q, Yan X, Wang J, Chen Y, Wang X, Li C, et al. Abnormalities of White Matter Microstructure in

Unmedicated Obsessive-Compulsive Disorder and Changes after Medication. *PLoS One*.2012;7(4): e35889.

Fontenelle LF, Harrison BJ, Yücel M, Pujol J, Fujiwara H, Pantelis C. Is there evidence of brain white-matter abnormalities in obsessive-compulsive disorder?: a narrative review. *Topics in Magnetic Resonance Imaging*.2009;20(5): 291-8.

Friedlander L, Desrocher M. Neuroimaging studies of obsessive-compulsive disorder in adults and children. *Clinical psychology review*.2006;26(1): 32.

Garber HJ, Ananth JV, Chiu LC, Griswold VJ, Oldendorf WH. Nuclear magnetic resonance study of obsessive-compulsive disorder. *The American journal of psychiatry*.1989;146(8): 1001-5.

Garibotto V, Scifo P, Gorini A, Alonso CR, Brambati S, Bellodi L, et al. Disorganization of anatomical connectivity in obsessive compulsive disorder: a multi-parameter diffusion tensor imaging study in a subpopulation of patients. *Neurobiology of disease*.2010;37(2): 468.

Gong G, He Y, Concha L, Lebel C, Gross DW, Evans AC, et al. Mapping anatomical connectivity patterns of human cerebral cortex using in vivo diffusion tensor imaging tractography. *Cerebral Cortex*.2009;19(3): 524-36.

Gong G, Rosa-Neto P, Carbonell F, Chen ZJ, He Y, Evans AC. Age-and gender-related differences in the cortical anatomical network. *The Journal of Neuroscience*.2009;29(50): 15684-93.

Goodman WK, Price LH, Rasmussen SA, Mazure C, Fleischmann RL, Hill CL, et al. The Yale-Brown obsessive compulsive scale: I. Development, use, and reliability. *Archives of general psychiatry*.1989;46(11): 1006.

Hagmann P, Cammoun L, Gigandet X, Meuli R, Honey CJ, Wedeen VJ, et al. Mapping the structural core of human cerebral cortex. *PLoS biology*.2008;6(7): e159.

Hamilton M. The assessment of anxiety states by rating. *British journal of medical psychology*.1959;32(1): 50-5.

Hamilton M. A rating scale for depression. *Journal of neurology, neurosurgery, and psychiatry*.1960;23(1): 56.

He Y, Evans A. Graph theoretical modeling of brain connectivity. *Current opinion in neurology*.2010;23(4): 341-50.

Horwath E, Weissman MM. The epidemiology and cross-national presentation of obsessive-compulsive disorder. *Psychiatric Clinics of North America*.2000;23(3): 493-507.

Humphries MD, Gurney K, Prescott TJ. Is there an integrative center in the vertebrate brain-stem? A

robotic evaluation of a model of the reticular formation viewed as an action selection device. *Adaptive Behavior*.2005;13(2): 97-113.

Iturria-Medina Y, Sotero RC, Canales-Rodríguez EJ, Alemán-Gómez Y, Melie-García L. Studying the human brain anatomical network via diffusion-weighted MRI and Graph Theory. *Neuroimage*.2008;40(3): 1064.

Jang JH, Kim J-H, Jung WH, Choi J-S, Jung MH, Lee J-M, et al. Functional connectivity in fronto-subcortical circuitry during the resting state in obsessive-compulsive disorder. *Neuroscience letters*.2010;474(3): 158-62.

Kim J-J, Lee MC, Kim J, Kim IY, Kim SI, Han MH, et al. Grey matter abnormalities in obsessive—compulsive disorder Statistical parametric mapping of segmented magnetic resonance images. *The British Journal of Psychiatry*.2001;179(4): 330-4.

Kitamura H, Shioiri T, Kimura T, Ohkubo M, Nakada T, Someya T. Parietal white matter abnormalities in obsessive - compulsive disorder: a magnetic resonance spectroscopy study at 3 - Tesla. *Acta Psychiatrica Scandinavica*.2006;114(2): 101-8.

Kwon JS, Jang JH, Choi J-S, Kang D-H. Neuroimaging in obsessive-compulsive disorder. *Expert Review of Neurotherapeutics*. 2009;9:255-69.

Latora V, Marchiori M. Efficient behavior of small-world networks. *Physical review letters*.2001;87(19): 198701.

Li F, Huang X, Yang Y, Li B, Wu Q, Zhang T, et al. Microstructural brain abnormalities in patients with obsessive-compulsive disorder: diffusion-tensor MR imaging study at 3.0 T. *Radiology*.2011;260(1): 216-23.

Li Y, Liu Y, Li J, Qin W, Li K, Yu C, et al. Brain anatomical network and intelligence. *PLoS computational biology*.2009;5(5): e1000395.

Lochner C, Fouché J-P, du Plessis S, Spottiswoode B, Seedat S. Evidence for fractional anisotropy and mean diffusivity white matter abnormalities in the internal capsule and cingulum in patients with obsessive—compulsive disorder. *Journal of psychiatry & neuroscience: JPN*.2012;37(3): 193.

Machlin SR, Harris GJ, Pearlson GD, Hoehn-Saric R, Jeffery P, Camargo E. Elevated medial-frontal cerebral blood flow in obsessive-compulsive patients: a SPECT study. *The American journal of psychiatry*.1991;148(9): 1240.

Martinot J, Allilaire J, Mazoyer B, Hantouche E, Huret J, Legaut - Demare F, et al. Obsessive - compulsive disorder: A clinical, neuropsychological and positron emission tomography study. *Acta Psychiatrica Scandinavica*.1990;82(3): 233-42.

Maslov S, Sneppen K. Specificity and stability in topology of protein networks. *Science Signaling*.2002;296(5569): 910.

Mataix-Cols D, Wooderson S, Lawrence N, Brammer MJ, Speckens A, Phillips ML. Distinct neural correlates of washing, checking, and hoarding symptom dimensions in obsessive-compulsive disorder. *Archives of general psychiatry*.2004;61(6): 564.

Monzani B, Rijdsdijk F, Iervolino AC, Anson M, Cherkas L, Mataix - Cols D. Evidence for a genetic overlap between body dysmorphic concerns and obsessive - compulsive symptoms in an adult female community twin sample. *American Journal of Medical Genetics Part B: Neuropsychiatric Genetics*.2012;159(4): 376-82.

Mori S, Crain BJ, Chacko V, Van Zijl P. Three - dimensional tracking of axonal projections in the brain by magnetic resonance imaging. *Annals of neurology*.1999;45(2): 265-9.

Mori S, van Zijl P. Fiber tracking: principles and strategies - a technical review. *NMR in Biomedicine*.2002;15(7 - 8): 468-80.

Nakamae T, Narumoto J, Shibata K, Matsumoto R, Kitabayashi Y, Yoshida T, et al. Alteration of fractional anisotropy and apparent diffusion coefficient in obsessive-compulsive disorder: a diffusion tensor imaging study. *Progress in neuro-psychopharmacology & biological psychiatry*.2008;32(5): 1221-6.

Oh JS, Jang JH, Jung WH, Kang DH, Choi JS, Choi CH, et al. Reduced fronto - callosal fiber integrity in unmedicated OCD patients: A diffusion tractography study. *Human brain mapping*.2012;33(10): 2441-52.

Posner MI, Petersen SE (1989). The attention system of the human brain, DTIC Document.

Sachdev P, Trollor J, Walker A, Wen W, Fulham M, Smith JS, et al. Bilateral orbitomedial leucotomy for obsessive - compulsive disorder: a single - case study using positron emission tomography. *Australian and New Zealand journal of psychiatry*.2001;35(5): 684-90.

Saito Y, Nobuhara K, Okugawa G, Takase K, Sugimoto T, Horiuchi M, et al. Corpus Callosum in Patients with Obsessive-Compulsive Disorder: Diffusion-Tensor Imaging Study1. *Radiology*.2008;246(2): 536-42.

Saxena S, Bota R, Brody A. Brain-behavior relationships in obsessive-compulsive disorder. *Seminars in clinical neuropsychiatry*.2001;6: 82.

Saxena S, Brody AL, Maidment KM, Dunkin JJ, Colgan M, Alborzian S, et al. Localized orbitofrontal and subcortical metabolic changes and predictors of response to paroxetine treatment in obsessive-compulsive disorder. *Neuropsychopharmacology*.1999;21(6): 683-93.

Shin YW, Yoo SY, Lee JK, Ha TH, Lee KJ, Lee JM, et al. Cortical thinning in obsessive compulsive disorder. *Human brain mapping*.2007;28(11): 1128-35.

Shu N, Liu Y, Li J, Li Y, Yu C, Jiang T. Altered anatomical network in early blindness revealed by diffusion tensor tractography. *PLoS One*.2009;4(9): e7228.

Shu N, Liu Y, Li K, Duan Y, Wang J, Yu C, et al. Diffusion tensor tractography reveals disrupted topological efficiency in white matter structural networks in multiple sclerosis. *Cerebral Cortex*.2011;21(11): 2565-77.

Sporns O, Tononi G, Kötter R. The human connectome: a structural description of the human brain. *PLoS computational biology*.2005;1(4): e42.

Sporns O, Zwi JD. The small world of the cerebral cortex. *Neuroinformatics*.2004;2(2): 145-62.

Susanna Carmona a NB, Mariana Rovira , Joan-Domingo Gispert, Joan-Carles Soliva , Marisol Prado , Josep Tomas , Antoni Bulbena , Oscar Vilarroya. Pediatric OCD structural brain deficits in conflict monitoring circuits: A voxel-based morphometry study. *Neuroscience Letters*.2007; 421: 218–23.

Szeszko PR, Ardekani BA, Ashtari M, Malhotra AK, Robinson DG, Bilder RM, et al. White matter abnormalities in obsessive-compulsive disorder: a diffusion tensor imaging study. *Archives of general psychiatry*.2005;62(7): 782-90.

Taylor S. Early versus late onset obsessive–compulsive disorder: evidence for distinct subtypes. *Clinical psychology review*.2011;31(7): 1083-100.

Tzourio-Mazoyer N, Landeau B, Papathanassiou D, Crivello F, Etard O, Delcroix N, et al. Automated anatomical labeling of activations in SPM using a macroscopic anatomical parcellation of the MNI MRI single-subject brain. *Neuroimage*.2002;15(1): 273-89.

Valente Jr AA, Miguel EC, Castro CC, Amaro Jr E, Duran F, Buchpiguel CA, et al. Regional gray matter abnormalities in obsessive-compulsive disorder: a voxel-based morphometry study. *Biological psychiatry*.2005;58(6): 479.

Van den Heuvel M, Stam C, Boersma M, HE HP. Small-world and scale-free organization of voxel-based resting-state functional connectivity in the human brain. *Neuroimage*.2008;43(3): 528.

van den Heuvel OA, Veltman DJ, Groenewegen HJ, Cath DC, van Balkom AJ, van Hartkamp J, et al. Frontal-striatal dysfunction during planning in obsessive-compulsive disorder. *Archives of general psychiatry*.2005;62(3): 301.

Wang J, Wang L, Zang Y, Yang H, Tang H, Gong Q, et al. Parcellation of small-world brain functional networks: A resting-state fMRI study. *Human brain mapping*.2009;30(5): 1511-23.

Watts DJ, Strogatz SH. Collective dynamics of 'small-world' networks. *nature*.1998;393(6684): 440-2.

Weissman MM, Bland RC, Canino GJ, Greenwald S. The cross national epidemiology of obsessive compulsive disorder: The Cross National Collaborative Group. *Journal of Clinical Psychiatry*.1994; 55(suppl)(5): 10.

Whiteside SP, Port JD, Deacon BJ, Abramowitz JS. A magnetic resonance spectroscopy investigation of obsessive-compulsive disorder and anxiety. *Psychiatry Research: Neuroimaging*.2006;146(2): 137-47.

Xia M, Wang J, He Y. BrainNet Viewer: A Network Visualization Tool for Human Brain Connectomics. *PLoS One*.2013;8(7): e68910.

Yoo S, Jang J, Shin YW, Kim D, Park HJ, Moon WJ, et al. White matter abnormalities in drug - naïve patients with obsessive - compulsive disorder: a Diffusion Tensor Study before and after citalopram treatment. *Acta Psychiatrica Scandinavica*.2007;116(3): 211-9.

Zai G, Bezchlibnyk YB, Richter MA, Arnold P, Burroughs E, Barr CL, et al. Myelin oligodendrocyte glycoprotein (MOG) gene is associated with obsessive - compulsive disorder. *American Journal of Medical Genetics Part B: Neuropsychiatric Genetics*.2004;129(1): 64-8.

Zalesky A, Fornito A, Harding IH, Cocchi L, Yücel M, Pantelis C, et al. Whole-brain anatomical networks: does the choice of nodes matter? *Neuroimage*.2010;50(3): 970.

Zhang T, Wang J, Yang Y, Wu Q, Li B, Chen L, et al. Abnormal small-world architecture of top-down control networks in obsessive-compulsive disorder. *Journal of psychiatry & neuroscience: JPN*.2011;36(1): 23.

**Table 1. Demographic and clinical characteristics of participants**

Characteristic	OCD patients	controls	<i>p</i> value
Age(years)	28.8±7.6(19-48)	27.7±7.7(18-45)	0.58
Gender	9/17	13/26	0.92
Education(years)	13.9±1.3	13.8±1.1	0.57
Brain Size(mm <sup>3</sup> )	1.16±0.16 x 10 <sup>7</sup>	1.20±0.18 x 10 <sup>7</sup>	0.36
Illness duration	4.6±3.5		
Total Y-BOCS score	25.3±5.8	NA	
Y-BOCS 1(Obsessive subscale)	14.5±2.6	NA	
Y-BOCS 2(Compulsive subscale)	10.8±5.6	NA	
HDRS score	9.2±4.46	NA	
HARS score	12.7±5.76	NA	

Abbreviation: Y-BOCS, Yale-Brown Obsessive Compulsive Scale.

HDRS, Hamilton Depression Rating Scale;

HARS, Hamilton Anxiety Rating Scale;

**Table 2 Cortical and subcortical region-of-interest defined in the study**

Index	Regions	Abbreviation	Index	Regions	Abbreviation
(1,2)	Precentral gyrus	PreCG	(47,48)	Lingual gyrus	LING
(3,4)	Superior frontal gyrus, dorsolateral	SFGdor	(49,50)	Superior occipital gyrus	SOG
(5,6)	Superior frontal gyrus, orbital part	ORBsup	(51,52)	Middle occipital gyrus	MOG
(7,8)	Middle frontal gyrus	MFG	(53,54)	Inferior occipital gyrus	IOG
(9, 10)	Middle frontal gyrus, orbital part	ORBmid	(55,56)	Fusiform gyrus	FFG
(11,12)	Inferior frontal gyrus, opercular part	IFGoperc	(57,58)	Postcentral gyrus	PoCG
(13,14)	Inferior frontal gyrus, triangular part	IFGtriang	(59,60)	Superior parietal gyrus	SPG
(15,16)	Inferior frontal gyrus, orbital part	ORBinf	(61,62)	Inferior parietal, supramarginal and angular gyri	IPL
(17,18)	Rolandic operculum	ROL	(63,64)	Supramarginal gyrus	SMG
(19,20)	Supplementary motor area	SMA	(65,66)	Angular gyrus	ANG
(21,22)	Olfactory cortex	OLF	(67,68)	Precuneus	PCUN
(23,24)	Superior frontal gyrus, medial	SFGmed	(69,70)	Paracentral lobule	PCL
(25,26)	Superior frontal gyrus, medial orbital	ORBsupmed	(71,72)	Caudate nucleus	CAU
(27,28)	Gyrus rectus	REC	(73,74)	Lenticular nucleus, putamen	PUT
(29,30)	Insula	INS	(75,76)	Lenticular nucleus, pallidum	PAL
(31,32)	Anterior cingulate and paracingulate gyri	ACG	(77,78)	Thalamus	THA
(33,34)	Median cingulate and paracingulate gyri	DCG	(79,80)	Heschl gyrus	HES
(35,36)	Posterior cingulate gyrus	PCG	(81,82)	Superior temporal gyrus	STG
(37,38)	Hippocampus HIP	HIP	(83,84)	Temporal pole: superior temporal gyrus	TPOsup
(39,40)	Parahippocampal gyrus	PHG	(85,86)	Middle temporal gyrus	MTG
(41,42)	Amygdala	AMYG	(87,88)	Temporal pole: middle temporal gyrus	TPOmid
(43,44)	Calcarine fissure and surrounding cortex	CAL	(89,90)	Inferior temporal gyrus	ITG
(45,46)	Cuneus	CUN			

**Note: The regions are listed according to a prior template obtained from an AAL atlas.**

**Table 3. Comparisons of the global network measures among the OCD and control groups**

	$S_p$	$E_{glob}$	$E_{loc}$	$l_p$	$C_p$	$\lambda$	$\gamma$	$\sigma$
Low-resolution network (L-AAL)								
OCD	256.9(41.4)	1.52(0.19)	2.42(0.27)	0.67(0.09)	0.36(0.02)	1.16(0.03)	4.32(0.38)	3.72(0.32)
Control	262.3(44.6)	1.59(0.20)	2.47(0.33)	0.64(0.08)	0.35(0.02)	1.15(0.03)	4.15(0.29)	3.63(0.28)
<i>t</i> value	- 1.20	- 2.32	- 1.17	2.30	1.63	2.08	2.26	1.46
<i>p</i> value	0.24	0.02	0.25	0.02	0.11	0.04	0.03	0.15

Abbreviation:  $S_p$ : Network Strength,  $E_{glob}$ :Network global efficiency,  $E_{loc}$ :Network local efficiency,  $l_p$ : the shortest path length,  $C_p$ : the clustering coefficient,  $\lambda$ : the normalized shortest path length,  $\gamma$ : the normalized clustering coefficient,  $\sigma$ : the small-worldness

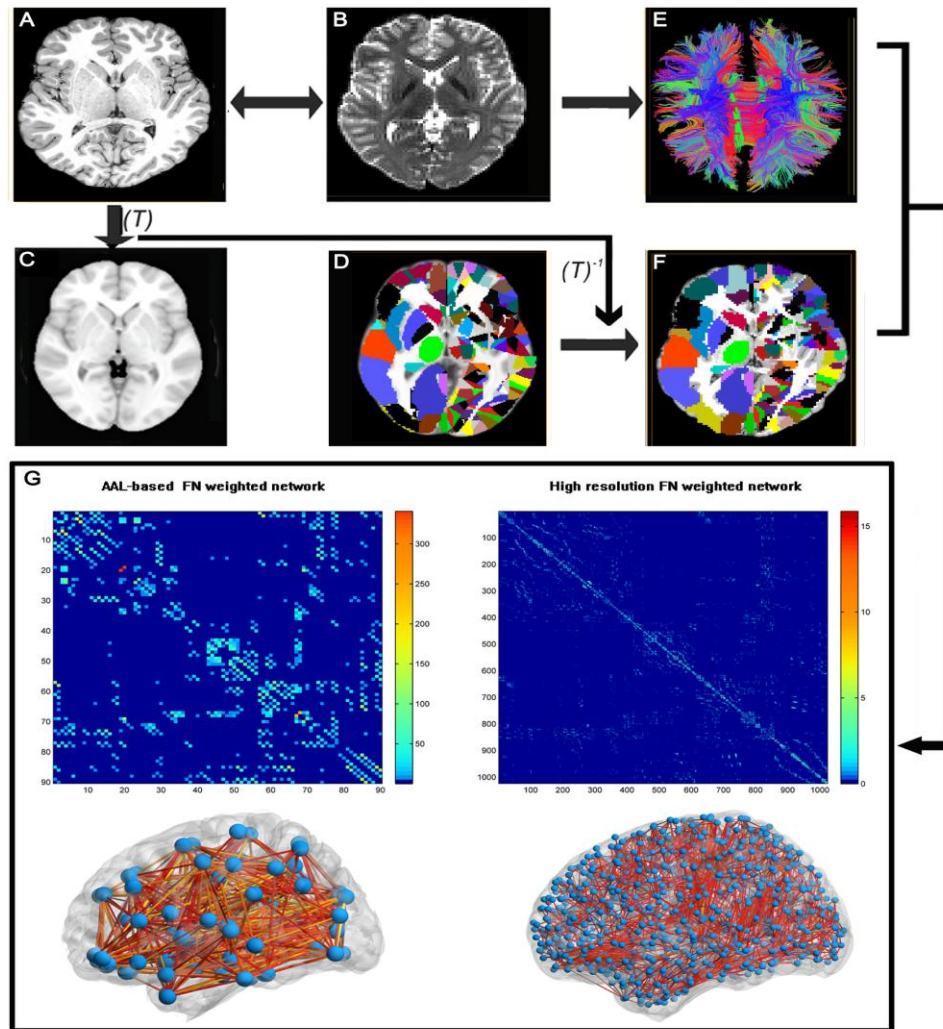


**Figure 1.** A flowchart for the construction of WM structural network by DTI. 1) The rigid co-registration from the native T1-weighted structural MRI (A) to S0 image in DTI native space (B) for each subject. 2) The nonlinear registration from the resultant structural MRI in DTI native space to the ICBM152T1 template in the MNI space (C), resulting in a nonlinear transformation ( $T$ ). 3) The application of the inverse transformation ( $T^{-1}$ ) to the automated anatomical labeling atlas and the AAL-based high resolution atlas in the MNI space (D), resulting in the subject-specific automated anatomical labeling mask and 1024 mask in the DTI native space (F). All registrations were implemented in the SPM8 package. 4) The reconstruction of all the WM fibers (E) in the whole brain using DTI deterministic tractography in DTIstudio. 5) The FN weighted networks of each subject (G) were created by computing the number of the fiber bundles that connected each pair of brain regions. The matrices and 3D representations (lateral view) of the mean WM structural networks of health control group in two different resolution were shown in the bottom panel. The nodes are located according to their centroid stereotaxic coordinates, and the edges are coded according to their connection weights. For details, see the Materials and Methods section.

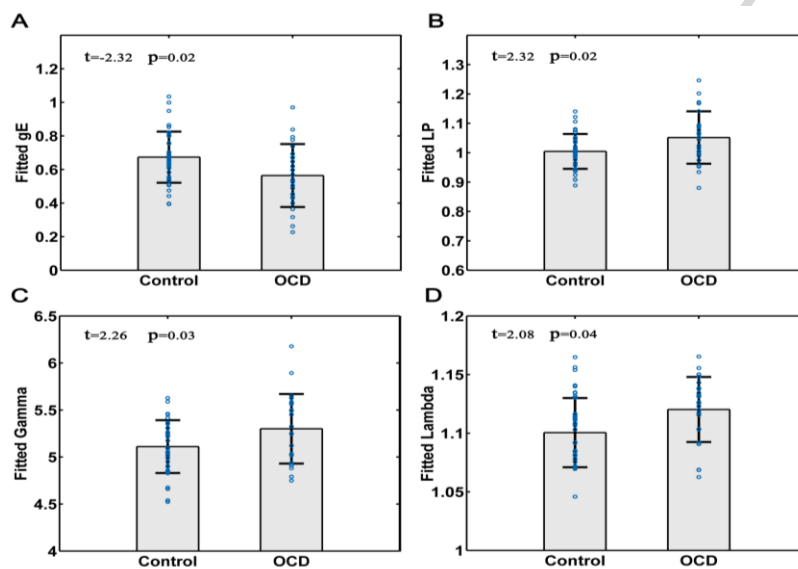


**Figure 2** Global topology measures of WM networks which show significant between-group differences. The bars represent the mean values, and error bars represent the SDs of the network parameters. The OCD group show significant decreased global efficiencies (gE) (A) and increased weighted shortest path length (LP) (B), normalized clustering coefficient (Gamma) (C) and normalized weighted shortest path length (Lambda) (D).

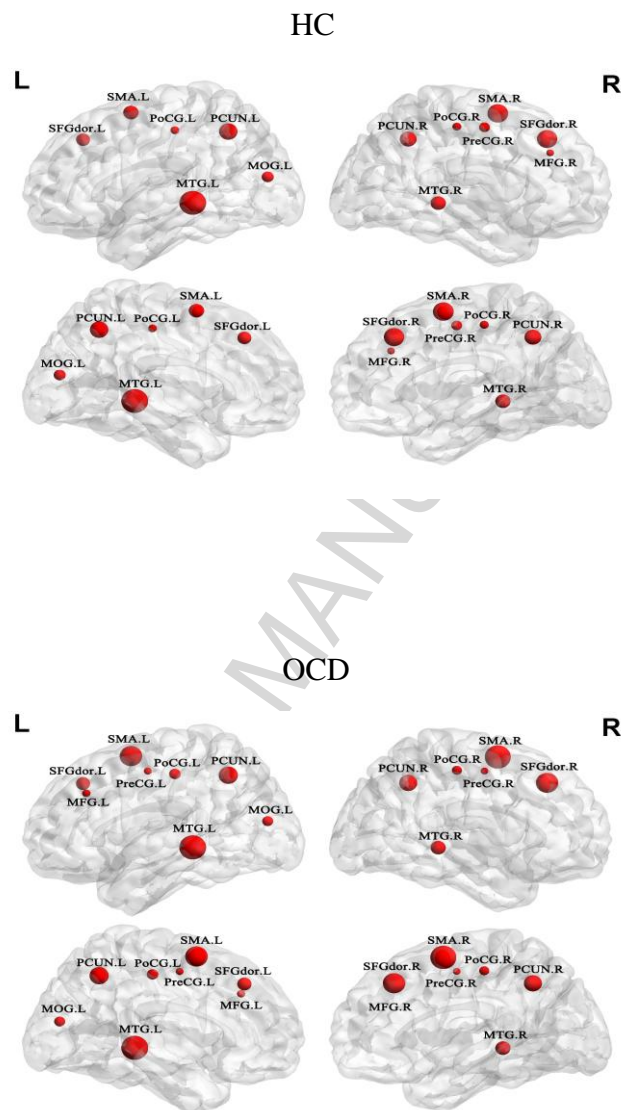


**Figure 3.** The hub region distributions in the WM structural networks of the HC and OCD groups. The hub nodes are shown in red with node sizes indicating their nodal efficiency values. The visualization used the Brain Net Viewer(Xia et al. 2013Xia et al. 2013).

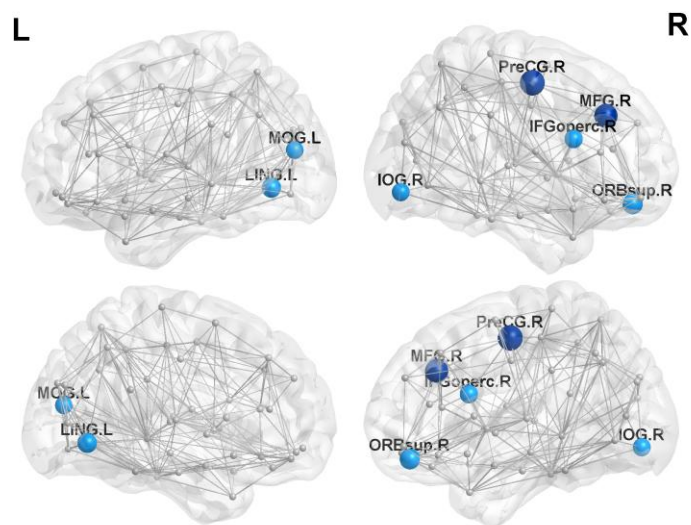


**Figure 4.** Regions with significant differences in nodal efficiency between OCD patients and NCs. Regions show significant reduced nodal efficiency in OCD patients in AAL network. Nodes colored in deep blue indicate the regions after FDR correction, nodes colored in light blue indicate the regions at an exploratory threshold ( $p < 0.01$ , uncorrected). The network edge was constructed by averaging the structure matrix of all participants.

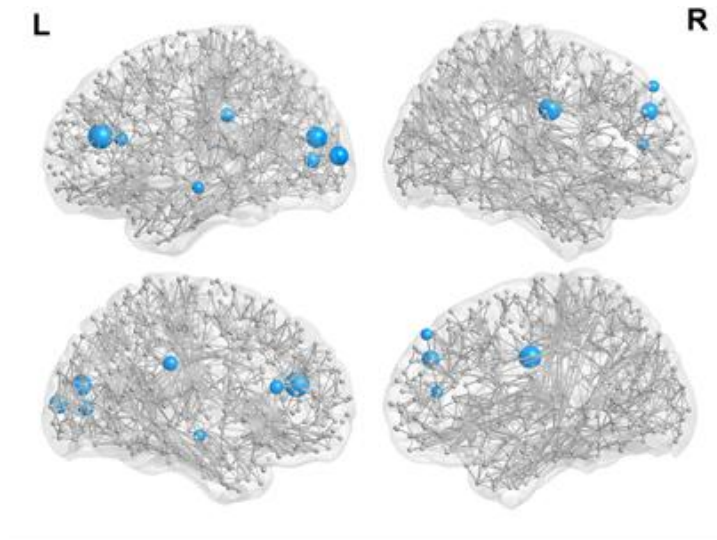


**Figure 5.** Regions show significant reduced nodal efficiency in OCD patients in high resolution network. ( $p < 0.01$ , uncorrected). The network edge was constructed by averaging the structure matrix of all participants.

ACCEPTED MANUSCRIPT

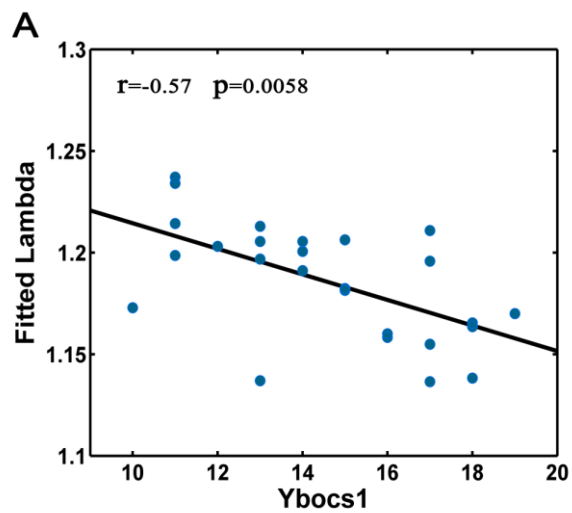


**Figure 6** The Correlation between the Network metrics and Y-BOCS scores in OCD patients. Plots showing the normalized weighted shortest path length (**Lambda**) of the network was significantly negatively correlated with Y-BOCS1.